Scientific Research Publishing

Open Journal of Geology, 2023, 13, 189-202
https://www.scirp.org/journal/ojg
ISSN Online: 2161-7589
ISSN Print: 2161-7570

Geochemistry of Layered Ultramafic Rocks in J.C. Pura Schist Belt, Dharwar Craton, Karnataka, India

S. Santhosh, B. G. Dayanand, B. C. Prabhakar

Department of Geology, Bangalore University, Bangalore, India
Email: geosantu@gmail.com, dayanandbg22@gmail.com, bcprabhakar@rediffmail.com

How to cite this paper: Santhosh, S., Dayanand, B.G. and Prabhakar, B.C. (2023) Geochemistry of Layered Ultramafic Rocks in J.C. Pura Schist Belt, Dharwar Craton, Karnataka, India. *Open Journal of Geology*, **13**, 189-202.
https://doi.org/10.4236/ojg.2023.132009

Received: January 9, 2023
Accepted: February 25, 2023
Published: February 28, 2023

Abstract

The Jayachamarajapura schist belt in western Dharwar craton, southern India, is predominantly an ultramafics dominant terrain. These rocks have been extensively metamorphosed and altered to serpentinite. The komatiite nature of ultramafics is conspicuous. In most of the areas of the belt these ultramafics are massive in nature. However, some of the ultramafic units show layered nature. But, their outcrops are encompassed within the massive komatiitic bodies. These komatiitic ultramafics are predominantly Mg-rich in nature. The layered rocks are also Mg-rich, and their field setting and geochemistry suggest their intermittent occurrence as sills, during the differentiation of peridotitic magma. The layered rocks, which have been intensely serpentinisation show homogenous nature. They are almost wholly made of serpentine with occasional relics of pyroxene. Secondary carbonate mineral is often noticed. Their higher MgO content indicates Mg-rich ultramafic magmatism during Archaean orogeny.

Keywords

Western Dharwar Craton, Layered Sequences, Komatiite, J.C. Pura Belt

1. Introduction

Layered igneous intrusions occur in several parts of the cratonic blocks and have greater magmatic and metallogenic significance. They also range in spatial extent from huge provinces like the Bushveld igneous complex [1] to small basins like Nuggihalli belt [2]. They are predominantly ultramafic in nature, with extremely localized differentiation to produce varied lithosections. Well differentiated layered intrusive bodies confine to a deep-seated environment [3], whereas several extensive komatiitic sequences sporadically contain intrusive sills formed

during episodic magmatism. These layered bodies are also the sites of several metalliferous deposits like chromite-magnetite, Ni-Cu deposits, and PGEs like that of Bushveld Igneous Complex of South Africa [4], the great dyke of Zimbabwe [5], Monchegorsk Complex of Russia [6], Stillwater complex of U.S.A. [4], Penikat Layered Complex of Finland [7], and others which have similar geological setting and are of greater importance for exploration. Indian occurrences of layered sequences are relatively less, and a few are confined to older cratonic terrains. Sittampundi in Tamilnadu [8], Boula Naushai in Orissa [9], Nuggiahalli in Karnataka [10], Naga hills in Manipur [11], Kondapalli in Andhra Pradesh [12] are some of them. However, their complete metallogenic potential is still to be realized. The presence of PGEs in ultramafic-mafic massifs has traditionally been linked to deep-seated magmatism [13]. PGE mineralization occurs mostly in thinly stratified intrusions as in Bushveld Igneous Complex [14]. They are also loaded with gold, copper-nickel sulfides, chromium oxides, and PGEs. PGM frequently mineralizes when base metallic sulfides and oxide silicates come into contact or when incorporated into the sulfides themselves.

2. Geology of the J.C. Pura Belt

The J.C. Pura belt in the western Dharwar craton (WDC) contains one of the oldest assemblies of gneisses and greenstone rocks, dating back to 3.23 Ga [15]. It is a NW-trending strip of greenstone komatiitic rich ultramafic rocks (**Figure 1**), which is part of the older Sargur Group [15] [16]. It is dominated by ultramafic terrain with Komatiitic features, which are serpentinized, chloritized, and carbonatized [17]. The komatiitic rock is contemporary with the TTG accretion adjacent to it. The komatiites of the J.C. Pura schist belt have undergone low-grade metamorphism, ranging from greenschist to lower amphibolite facies [18]. Serpentinization of essential minerals such as olivine and pyroxene has been common throughout the belt, particularly in dunite-rich layers. Mesoscale rocks are distinguished from related komatiitic rocks by their dense layering, which indicates their occurrence at a deeper level, probably as sills. Numerous stratified bodies of dunite, peridotite, and pyroxenite are found as sills across the widespread komatiites **Figure 2(a)**. Distinct color bands of olive green dunite, buff-colored peridotite, and pinkish brown pyroxenite demonstrate layering. The dimensions of these strata range from 2 cm to well over half a meter. Due to their monomineral composition, dunite and pyroxenite bearing strata exhibit uniform outcrop surface expression, whereas peridotite layers exhibit heterogeneous surface expression. Peridotite is composed of olivine and pyroxene cumulates, and due to the increased resistance of pyroxene cumulates to weathering, they stand out prominently in outcrops. The contact between layers is distinct, and interaction between dunite and pyroxenite and peridotite and pyroxenite are visible. The sharp contacts may be primarily the result of episodic injection of undifferentiated to slightly differentiated magma pulses that cooled and solidified without undergoing significant fractional crystallization [19]. Magnetite bands associated with chromite are also noticed in the layered sequences (**Figure 2(b)**). In order

to define layered komatiite mineralogy, secondary processes and characterize the possible elemental (major, trace including REE and PGE) compositions and in turn to identify their possible hosting of PGE's, this study has been carried out.

3. Materials and Methods

Mafic and ultramafic samples were collected from the J.C. Pura schist belt during field investigation. Six layered peridotite samples were chosen, and petrographic sections were prepared to examine the various mineral phases. These samples were also subjected to XRF analysis. The analysis produced values for the major and trace elements (Table 1), using which the geochemical plots are prepared to comprehend their geochemical relationship.

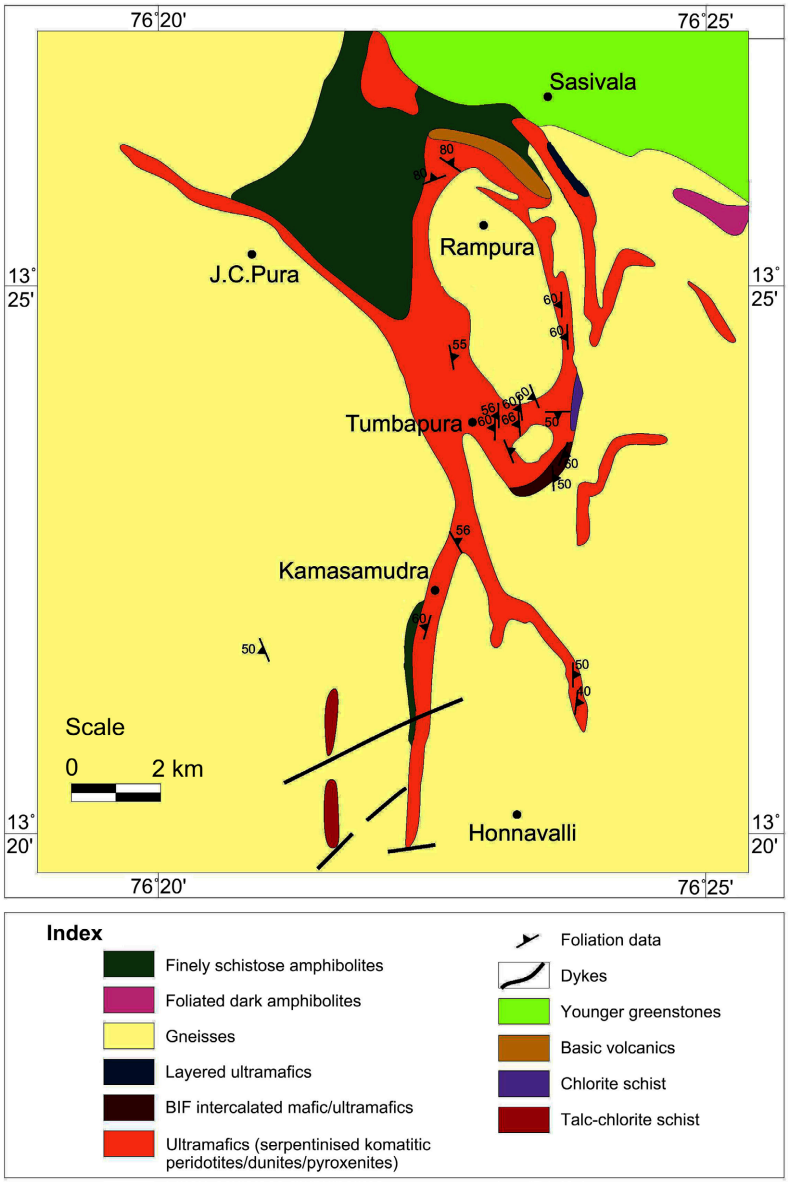

Figure 1. Geological map of J.C. Pura schist belt.

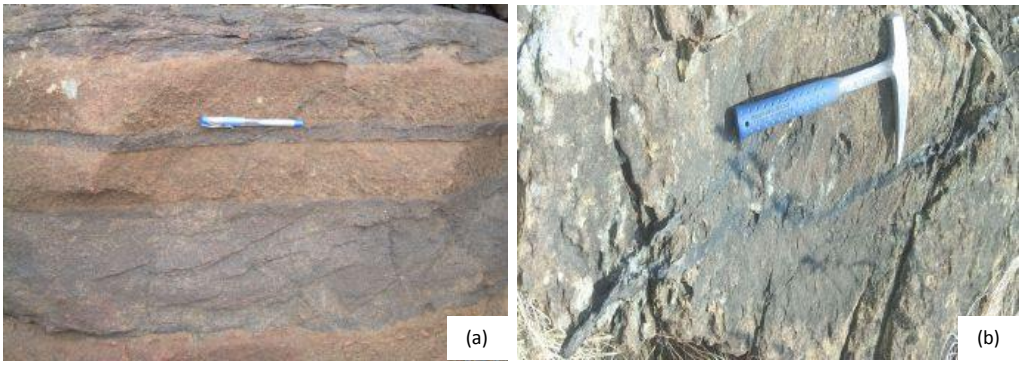

Figure 2. Field images. (a): Peridotite-pyroxenite-dunite layering showing sharp contact; (b): magnetite band in pyroxenite.

Table 1. Geochemical analytical data.

Sample No	JCU 87	JCU 88	JCU 88 A	JCU 88 B	JCU 88 C	JCU 88 D
SiO_2	44.3	44.07	46.58	44.85	47.93	46.04
TiO_2	0.71	0.83	0.65	0.64	0.71	0.37
Al_2O_3	2.39	3.13	1.30	3.29	2.81	2.91
Fe_2O_3	11.52	11.26	12.07	11.98	13.21	12.55
MnO	0.25	0.29	0.23	0.3	0.19	0.19
MgO	32.59	30.13	25.42	34.38	24.12	24.91
CaO	3.35	5.73	6.14	4.14	5.71	7.21
Na_2O	0.16	0.18	2.23	0.17	0.23	0.27
K_2O	0.02	0.03	0.04	0.03	0.04	0.05
P_2O_5	0.02	0.02	0.02	0.02	0.04	0.02
TOTAL	95.31	95.67	94.68	99.8	94.99	94.52
Sc	13.92	11.03	26.64	17.27	23.09	26.42
Cr	3992.08	1726.21	2028.18	1812.29	1328.38	2431.31
Ni	1651.55	1464.27	1015.88	1430.4	1311.17	1195.51
Rb	0.00	1.87	1.51	2.8	0.79	1.19
Sr	24.30	21.11	21.22	20.08	22.79	25.15
Y	4.45	3.56	5.1	3.58	9.19	9.11
Zr	4.50	6.38	4.85	2.9	7.08	9.3
Nb	1.85	1.72	2.17	1.58	0.76	2.85
Ba	18.23	23.02	24.39	24.02	35.11	44.39
Cu	21.43	36.62	34.39	22.41	31.31	18.98
La	16.74	6.93	3.3	8.53	32.24	15.8
Ce	4.62	1.77	1.21	2.58	2.38	1.7
Nd	6.72	20.03	18.57	25.7	5.86	15.93
Co	67.16	64.68	53.65	67.09	53.27	49.58
Pb	12.33	11.49	12.02	11.97	13.28	10.9
Th	0.52	0.41	0.44	0.53	0.4	0.57
V	69.55	72.71	74.86	74.5	83.08	90.76
Zn	148.17	131.8	103.53	128.44	73.94	81.59
Ga	4.50	1.11	0.33	7.25	1.93	1.21
U	0.00	0	0.04	0.02	0	0.03

4. Results

Petrography

Petrographic studies of the study area reveal the ubiquitous serpentinisation of most rocks. They also display distinct textural patterns. Dunites and peridotites are fine-grained and serpentinized, so the original olivine grains are completely obliterated. Primary minerals in layered strata, particularly olivine and pyroxene bearing ones, show serpentinization with fractured small grains. Pyroxene crystals are better preserved in peridotite strata, whereas olivine crystals are highly serpentinized (**Figure 3(a)**). The cumulus texture at places indicates the early growth of pyroxenes, but they are also completely serpentinized. The coarse pyroxene cumulates have a complex texture. They sometimes comprise sub-cumulus-like serpentinized masses encircled by thick iron oxide rims. All stratified lithologies contain altered subhedral to euhedral carbonate grains (**Figure 3(b)**). Pyroxene is relatively better retained than olivine in some peridotitic verities. Pyroxenites bearing layered sequences have a high carbonate content. Disseminated sulfide minerals are also observed in layered dunite-peridotites. Sulfides are seen as dispersed grains both as independent grains and with oxide phases. Dissiminated pyrrhotite and pentlandite grains exist in exsolution form (**Figure 3(c)**). The exsolved magnetite-ilmenite is the most common phase (**Figure 3(d)**). Pentlandite, chalcopyrite, and pyrite are multiphase sulfide associations (**Figure 3(e)**). Oxide mineral aggregates are present in gabbro (**Figure 3(f)**). These sulfide associations might reflect as the possible PGE associations.

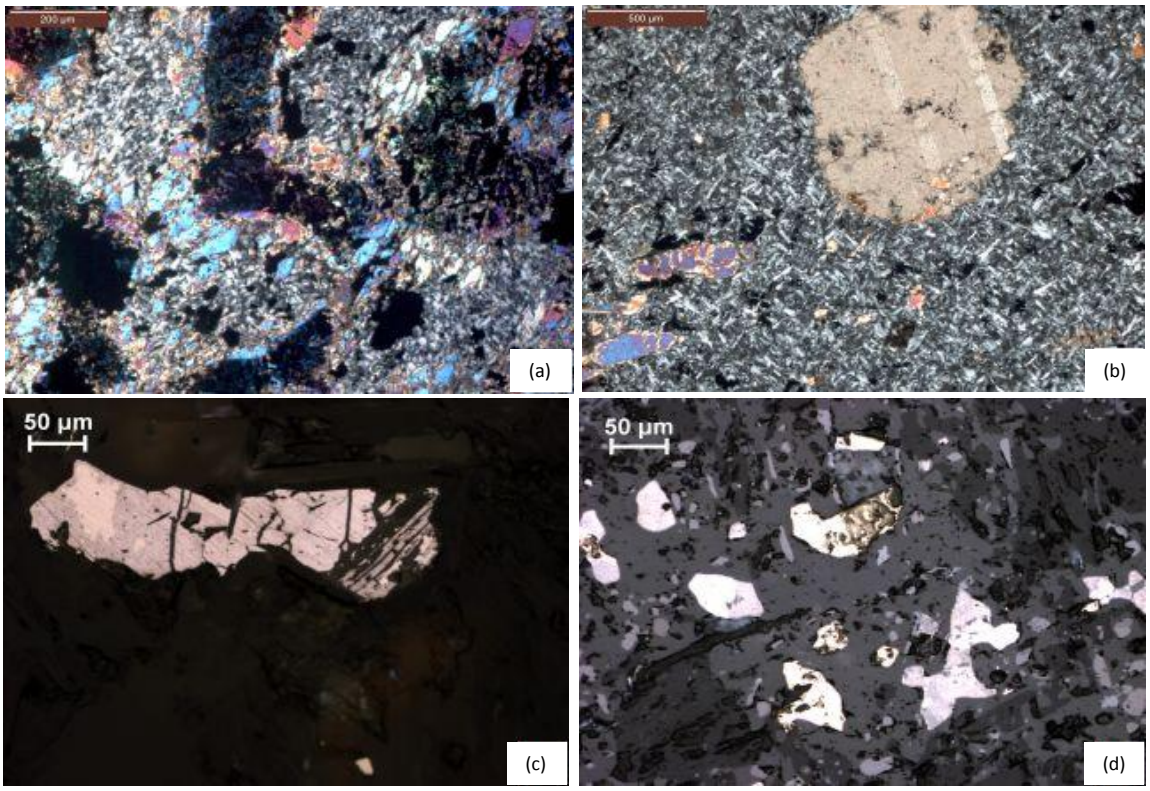

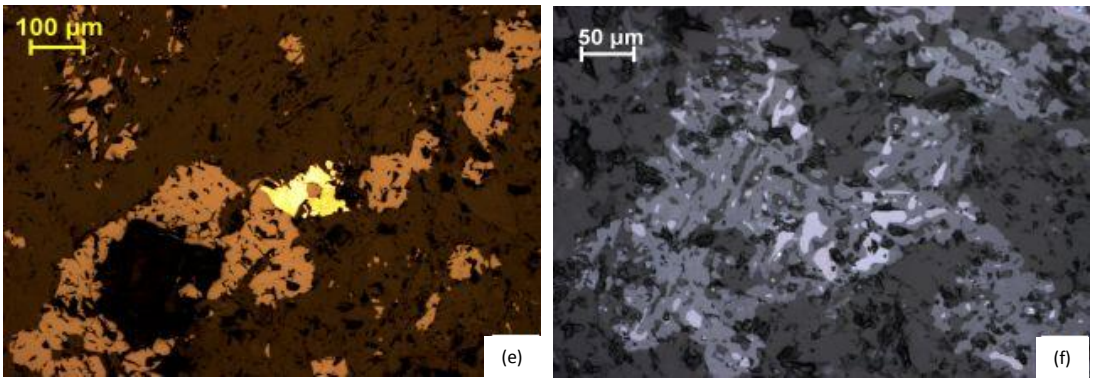

Figure 3. Petrographic images. (a): Serpentinised minerals surrounded by thick rims of iron oxide; (b): serpentine and carbonate association in the layered peridotite; (c): disseminated grains of pyrrhotite showing exolved phase of pentalandite; (d): exolved sulphides in magnetite; (e): association of chalcopyrite-pyrite-pyrrhotite and pentalandite; (f): oxide mineral aggregate in gabbro.

5. Discussion

Geochemistry

The Komatiites of Archaean and early Proterozoic greenstone belts have high MgO (>18%) but low K_2O (0.5%), SiO_2 (40% - 45%), CaO and Na_2O (2% combined), and low Ba, Cs, Rb (incompatible elements) with enrichment of LILE 1000 ppm [20] and with high Ni (>400 ppm), Cr (>800 ppm), Co (>150 ppm). The primary differentiation between komatiites and komatiite basalts is based on the MgO concentrations established by Arndt and Nisbet [21]. The greater MgO level indicates extrusive ultramafic flows and affiliation to the komatiitic suite. The Western Dharwar Craton's whole-rock geochemistry of komatiites indicates the depletion of diverse mantle sources [22]. In the present study, the layered peridotites of J. C. Pura show a homogenous komatiitic composition (24.12 - 32.59 wt% MgO), which is reflected in (**Figure 4(a)**). However, Komatiite having slightly greater SiO_2 (often about 50 wt%), are comparable to komatiitic basalt and pillowed komatiitic basalts as shown from the Barberton belt [23]. The layered komatiitic rocks of the study area have a relatively high MgO concentration. However, the greater MgO content is at odds with the fact that olivine has been entirely serpentinized in most of the locations in the present study, making it difficult to draw a comparison between the higher olivine concentration (modal olivine) and the higher MgO content. AFM diagrams (**Figure 4(b)**) and (Fe_2O_3 + TiO_2)-Al_2O-MgO (Jensen plot) reveal their strong komatiitic affinity (**Figure 4(c)**). All samples fall in komatiite field. Olivine acts as a regulator for immobile elements like MgO and Al_2O_3, ensuring that they remain chemically stable through hydrothermal alterations, metamorphism, and secondary processes. TiO_2 also behaves as an immobile component, although in this case, it is slightly lower (0.37 - 0.83 wt%) than in other komatiitic locations. Almost all samples had a moderate quantity of Al_2O_3 (1.30 - 3.13 wt%, with the majority being around 2.7%), which is comparable to the alumina-poor komatiitic basalts of the Barberton region. Thus, when the trends of the three elements, SiO_2, Al_2O_3, and TiO_2, which be-

have as stationary elements, are plotted on variation diagrams, they generate moderate trends [24]. Fresh komatiites from Zvishavane, Zimbabwe, exhibit similar characteristics [25].

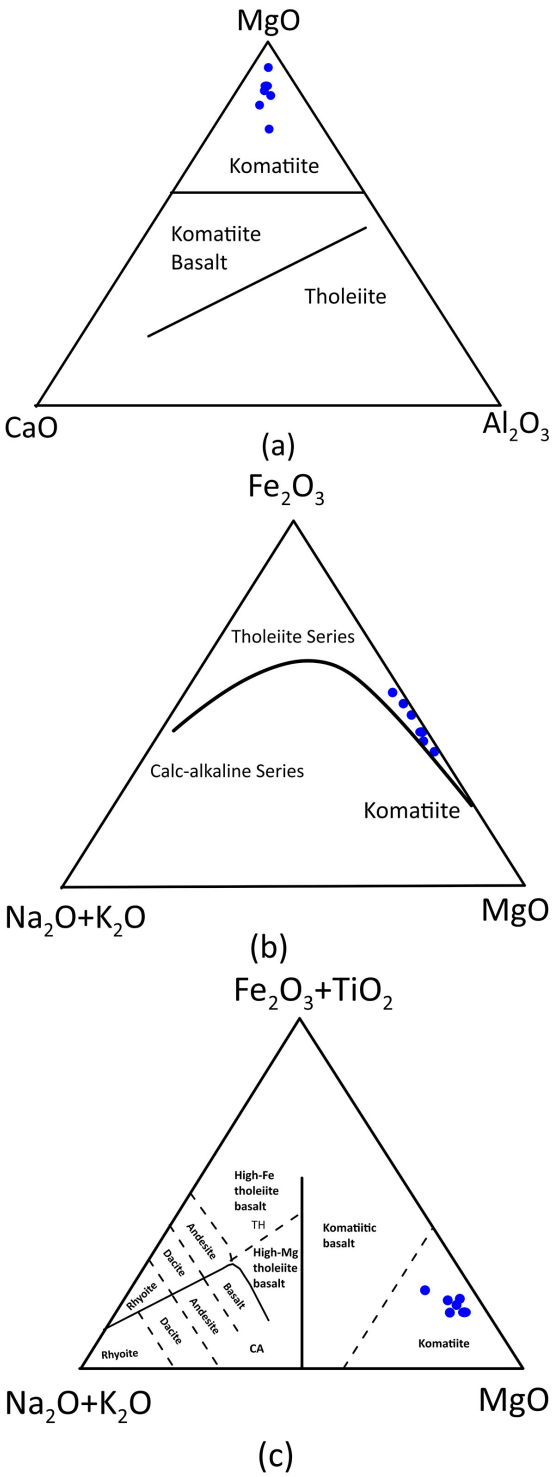

Figure 4. Terenary plots. (a): CaO-MgO-Al_2O_3 ternary plot showing Komatiite composition; (b): AFM diagram; (c): Jensen cation diagram.

Arndt [24] noted a substantial variation in trace element concentration and distribution in komatiitic rocks. The mobility and compatibility of various elements determine the amount of the elements and how they behave in komatiitic rocks. Elemental mobility can be determined by looking at the trace elements or their ratios with oxides or their ratios [26]. A strong correlation between two variables is frequently interpreted as an indication of immobility. REE distribution in the layered komatiites of J.C. Pura exhibits low concentration and nearly flat patterns, revealing their depleted mantle source and poor fractionation of the ultramafic magma [27]. As most REE and high-field strength elements are impervious to hydrothermal solutions, they tend to maintain their concentration level in undisturbed rocks, despite the fact that the rocks have been altered. An abundance of plumes of origin can be seen in the Nb/Y and Zr/Y diagrams (**Figure 5(a)**). The komatiites have homogeneous Al_2O_3/TiO_2, (Gd/Yb)N ratios (**Figure 5(b)**, **Figure 5(c)**), and have Al-depleted character (CaO/Al_2O_3 = 1.25 - 4.72 and Al_2O_3/TiO_2 = 2 - 7.86). Na_2O and K_2O show mild dispersion, indicating mobility during secondary processes. The key element oxides of komatiites (SiO_2, Al_2O_3, TiO_2, Fe_2O_3, CaO) show moderate to strong negative correlation (**Figure 6**). Ni has a positive association with MgO, indicating olivine fractionation, while Cr values demonstrate olivine, pyroxene, and chromite fractionation (**Figure 7**). Cr and Ni traces have high anomalous values. Nevertheless, Pb displays a substantial negative anomaly. This scenario has been linked to garnet or majorite fractionation during partial melting in Barberton-type and Fe-rich Komatiites from Boston Creek [28]. Positive Zr and Hf anomalies in Munro-type komatiites were interpreted by the same authors as the result of a high-pressure phase, most likely perovskite, accumulating in their deep-mantle source. Cs, Sr, Ba, Th, U, Nb, Ta, La, Ce, Pb, Pr, Sr, Nd, Sm, Zr, Hf, Eu, and Ti exhibit a variable trend (either positive or negative), whereas Gd, Tb, Dy, Y, Ho, E, Tm, Yb, and Lu exhibit a nearly flat trend (**Figure 8**). All the elements, with the exception of Gd and Er, have low concentrations (**Figure 9**), which suggests that these rocks crystallized without much fractionation from the partial melting of the depleted mantle.

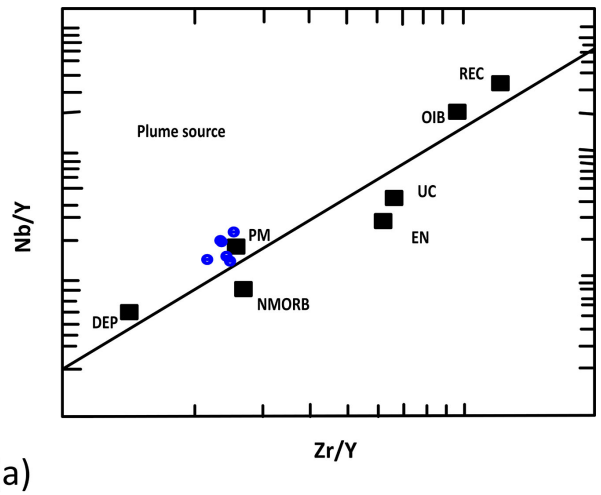

(a)

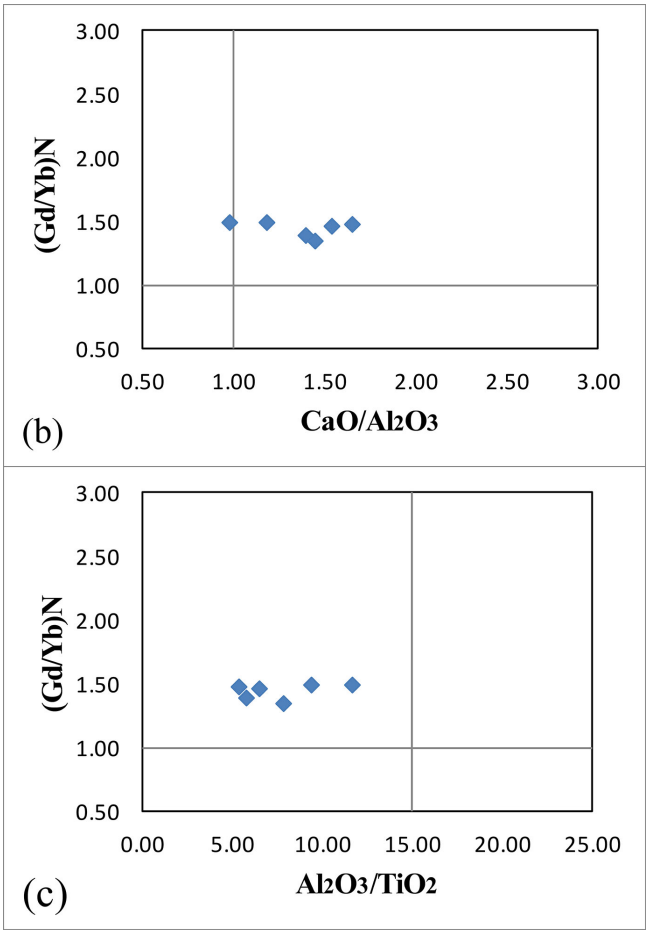

Figure 5. Binary plots. (a): Nb/Y versus Zr/Y diagram showing strong plume source; (b): (Gd/Yb)N vs. CaO/ Al_2O_3 plot; (c): (Gd/Yb)N vs. Al_2O_3/TiO_2 plot.

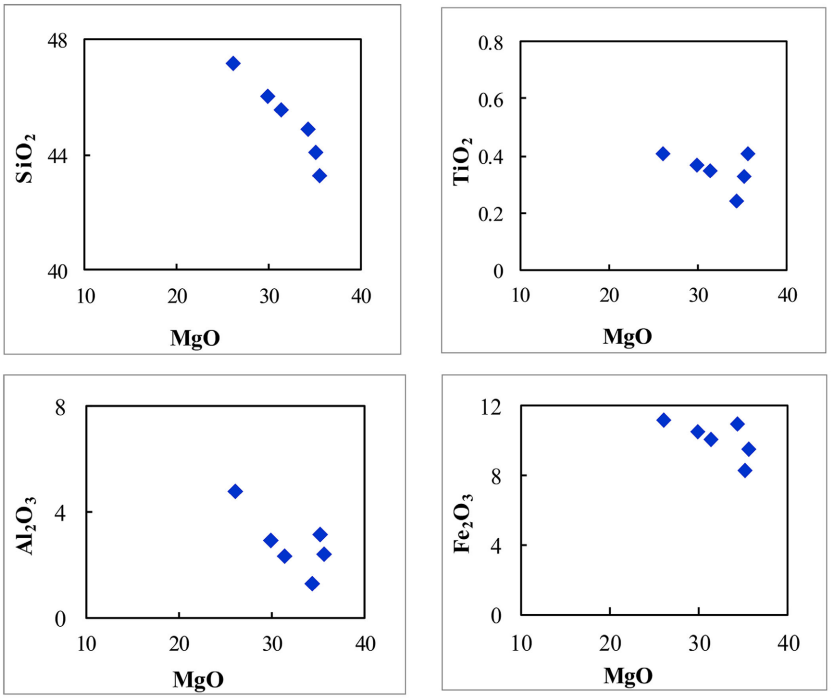

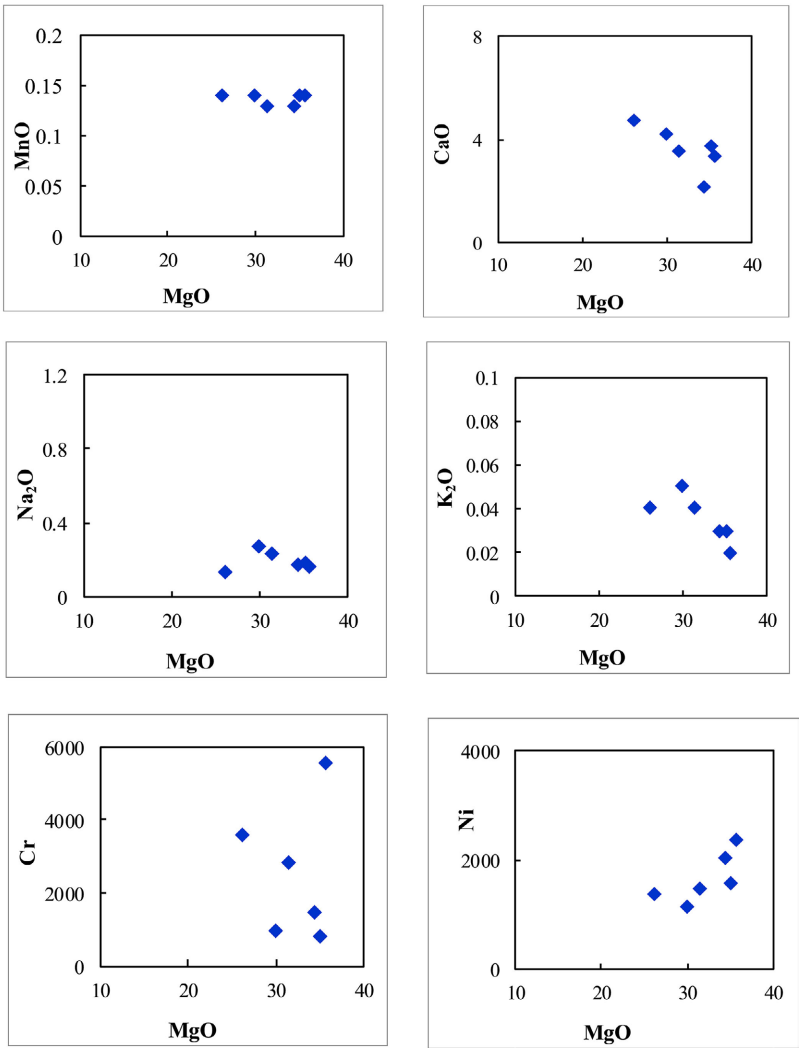

Figure 6. Harkers diagram of layered rocks in J.C. Pura belt.

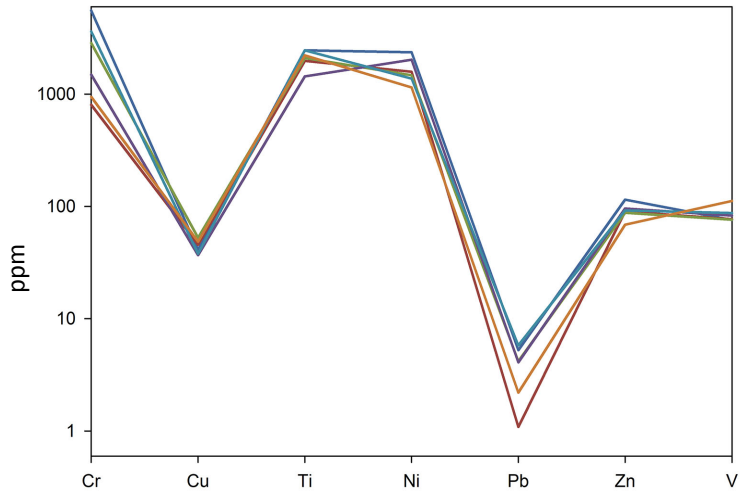

Figure 7. Spider diagram showing anomalous concentration for Cr, Ti and Ni, Pb, Zn, and V.

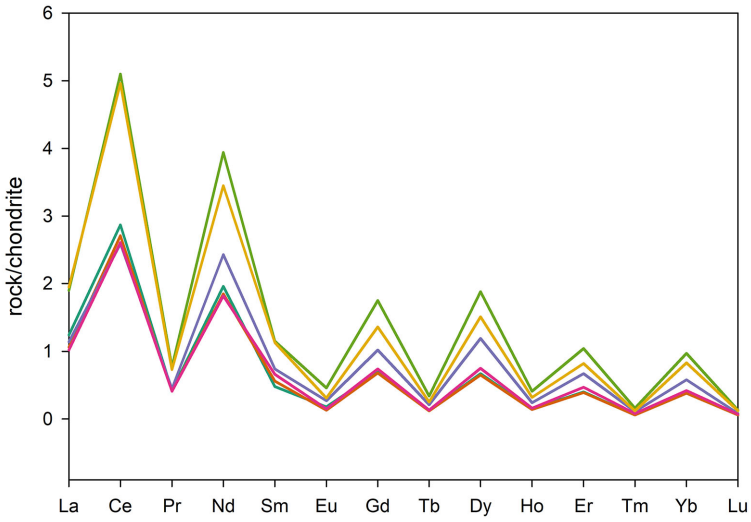

Figure 8. Chondrite-normalized REE patterns of komatiite from layered rock in J. C. Pura Belt.

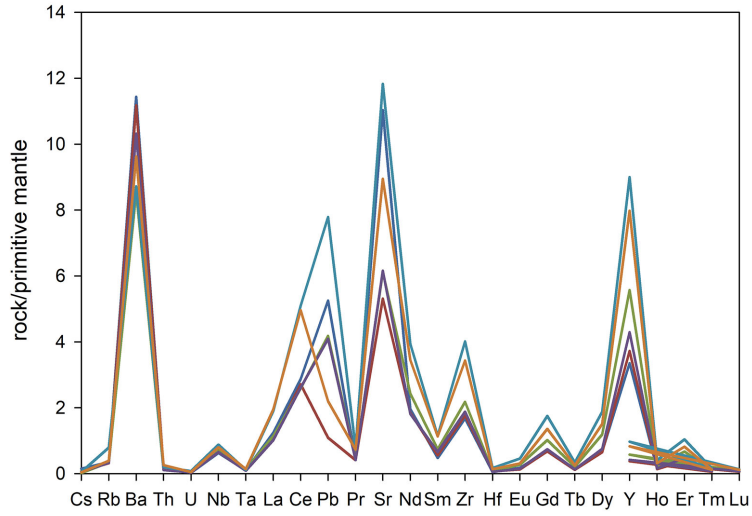

Figure 9. Primitive mantle-normalized multi element diagram (Sun and Mc Donough 1989).

6. Conclusions

The following conclusions can be drawn from the lithological, petrological, and geochemical investigation of the layered ultramafics of J.C. Pura schist belt:

1) Layered outcrops consisting magnetite, chromite, peridotite bandings constitute a significant feature in J. C. Pura schist belt, indicating sill like bodies intruded during the largely massive komatiite rich magmatic evolution.

2) Intense serpentinisation of these layered lithologies indicates large scale fluid activity at a later stage.

3) All the layered units are largely Mg rich and show strong komatiite nature, but are slightly alumina depleted.

4) Cr, Ni values are significantly high and were fractionated into Mg-rich phases.

5) It is inferred that these layered sequences have been derived from depleted mantle source.

6) The J.C. Pura shist belt has been identified as a possible zone hosting PGE mineralization based on geochemical trends and ore petrographic investigations.

Conflicts of Interest

The authors declare no conflicts of interest regarding the publication of this paper.

References

[1] Godel, B. (2015) Platinum-Group Element Deposits in Layered Intrusions: Recent Advances in the Understanding of the Ore Forming Processes. In: Charlier, B., *et al.*, Eds., *Layered Intrusions*, Springer, Berlin, 379-432. https://doi.org/10.1007/978-94-017-9652-1_9

[2] Rao, D.S., Babu, E.V.S.S.K., Balaram, V. and Vidyasagar, G. (2014) Geochemical Study of the Ultramafic-Mafic Plutonic and Volcanic Suites of the Nuggihalli Schist Belt, Western Dharwar Craton. *Conference GSI*, 107-126.

[3] Larsen, R.B., Grant, T., Sørensen, B.E., *et al.* (2018) Portrait of a Giant Deep-Seated Magmatic Conduit System: The Seiland Igneous Province. *Lithos*, **296-299**, 600-622. https://doi.org/10.1016/j.lithos.2017.11.013

[4] Godel, B., Barnes, S.J. and Maier, W.D. (2007) Platinum-Group Elements in Sulphide Minerals, Platinum-Group Minerals, and Whole-Rocks of the Merensky Reef (Bushveld Complex, South Africa): Implications for the Formation of the Reef. *Journal of Petrology*, **48**, 1569-1604. https://doi.org/10.1093/petrology/egm030

[5] Piña, R., Gervilla, F., Barnes, S. J., Oberthür, T. and Lunar, R. (2016) Platinum-Group Element Concentrations in Pyrite from the Main Sulfide Zone of the Great Dyke of Zimbabwe. *Mineralium Deposita*, **51**, 853-872. https://doi.org/10.1007/s00126-016-0642-3

[6] Sharkov, E.V. and Chistyakov, A.V. (2014) Geological and Petrological Aspects of Ni-Cu-PGE Mineralization in the Early Paleoproterozoic Monchegorsk Layered Mafic-Ultramafic Complex, Kola Peninsula. *Geology of Ore Deposits*, **56**, 147-168. https://doi.org/10.1134/S1075701514030040

[7] Barkov, A.Y., Fleet, M.E., Martin, R.F. and Halkoaho, T.A. (2005) A New Data on "Bonanza"-Type PGE Mineralization in the Kirakkajuppura PGE Deposit, Penikat Layered Complex, Finland. *The Canadian Mineralogist*, **43**, 1663-1686. https://doi.org/10.2113/gscanmin.43.5.1663

[8] Dhanendran, S., Nathan, N.P., Vijay Kumar, R., *et al.* (2014) Chromite and Sulphide Hosted PGE Mineralisation in Sittampundi Layered Anorthosite Complex, Tamil Nadu. *Conference GSI*, 1-8.

[9] Nayak, B., Sindern, S. and Wagner, T. (2021) Formation of Late-Stage Hydrothermal Mineralization in the Mesoarchean Boula-Nuasahi Ultramafic Complex, Odisha, India: Constraints from Arsenopyrite Geothermometry and Trace Element Data. *Ore Geology Reviews*, **139**, Article ID: 104482. https://doi.org/10.1016/j.oregeorev.2021.104482

[10] Mukherjee, R., Mondal, S.K. and Rosing, M.T. (2010) Compositional Variations in

the Mesoarchean Chromites of the Nuggihalli Schist Belt, Western Dharwar Craton (India): Potential Parental Melts and Implications for Tectonic Setting. *Contributions to Mineralogy and Petrology*, **160**, 865-885. https://doi.org/10.1007/s00410-010-0511-5

[11] Ghose, N.C. (2014) Occurrence of Native Gold and Gold-Silver Alloy in the Olivine Gabbro of Layered Cumulate Sequence of Naga Hills Ophiolite, India. *Current Science*, **106**, 1125-1130.

[12] Meshram, T. (2020) Mineralogical Variation in Platinum Group Element within Altered Chromitite of the Kondapalli Layered Igneous Complex (Southern India): Implication on Magmatic Evolution and Its Petrogenetic Significance. *Ore Geology Reviews*, **120**, Article ID: 103398. https://doi.org/10.1016/j.oregeorev.2020.103398

[13] Radomskaya, T.A., Glazunov, O.M., Vlasova, V.N. and Suvorova, L.F. (2017) Geochemistry and Mineralogy of Platinum Group Element in Ores of the Kingash Deposit, Eastern Sayan, Russia. *Geology of Ore Deposits*, **59**, 354-374. https://doi.org/10.1134/S107570151705004X

[14] Chistyakova, S., Latypov, R., *et al.* (2019) Merensky-Type Platinum Deposits and a Reappraisal of Magma Chamber Paradigms. *Scientific Reports*, **9**, Article No. 8807. https://doi.org/10.1038/s41598-019-45288-8

[15] Ramakrishnan, M., Venkata Dasu, S.P. and Kroner, A. (1994) Middle Archaean Age of Sargur Group by Single Grain Zircon Dating and Geochemical Evidence for the Clastic Origin of Metaquartzite from J.C. Pura Greenstone Belt, Karnataka. *Journal of the Geological Society of India*, **44**, 605-616.

[16] Venkata Dasu, S.P., Ramakrishnan, M. and Mahabaleswar, B. (1991) Sargur-Dharwar Relationship around the Komatiite-Rich J.C. Pura Greenstone Belt in Karnataka. *Journal of the Geological Society of India*, **38**, 577-592.

[17] Jayananda, M., Kano, T., Peucat, J.J. and Channabasappa, S. (2008) 3.35 Ga Komatiite Volcanism in the Western Dharwar Craton, Southern India: Constraints from Nd Isotopes and Whole-Rock Geochemistry. *Precambrian Research*, **162**, 160-179. https://doi.org/10.1016/j.precamres.2007.07.010

[18] Prabhakar, B.C. and Namrata, R. (2014) Morphology and Textures of Komatiite Flows of J.C. Pura Schist Belt, Dharwar Craton. *Journal of the Geological Society of India*, **83**, 1-8. https://doi.org/10.1007/s12594-014-0002-9

[19] Jayananda, M., Duraiswami, R.A., Aadhiseshan, K.R., Gireesh, R.V., Prabhakar, B.C., *et al.* (2016) Physical Volcanology and Geochemistry of Palaeoarchaean Komatiite Lava Flows from the Western Dharwar Craton, Southern India: Implications for Archaean Mantle Evolution and Crustal Growth. *International Geology Review*, **58**, 1569-1595. https://doi.org/10.1080/00206814.2016.1172350

[20] Philpotts, A. and Ague, J. (2009) Principles of Igneous and Metamorphic Petrology. Cambridge University Press, Cambridge. https://doi.org/10.1017/CBO9780511813429

[21] Viljoen, R.P. and Viljoen, M.J. (1969) The Geology and Geochemistry of the Lower Ultramafic Unit of the Onverwacht Group and a Proposed New Class of Igneous Rocks. *Geological Society of South Africa*, **2**, 55-85.

[22] Tushipokla and Jayananda, M. (2013) Geochemical Constraints on Komatiite Volcanism from Sargur Group Nagamangala Greenstone Belt, Western Dharwar Craton, Southern India: Implications for Mesoarchean Mantle Evolution and Continental Growth. *Geoscience Frontiers*, **4**, 321-340. https://doi.org/10.1016/j.gsf.2012.11.003

[23] Nesbitt, R.W., Sun, S.S. and Purvis, A.C. (1979) Komatiites; Geochemistry and Ge-

nesis. *The Canadian Mineralogist*, **17**, 165-186.

[24] Arndt, N. (2003) Komatiites, Kimberlites and Boninites. *Journal of Geophysical Research*, **108**, 2293-2304. https://doi.org/10.1029/2002JB002157

[25] Nisbet, E.G., Arndt, N.T., Bickle, M.J., Cameron, W.E., Chauvel, C., Cheadle, M., Hegner, E., Kyser, T.K., Martin, A., Renner, R. and Roedder, E. (1987) Uniquely Fresh 2.7 Ga Komatiites from the Belingwe Greenstone Belt, Zimbabwe. *Geology*, **15**, 1147-1150. https://doi.org/10.1130/0091-7613(1987)15<1147:UFGKFT>2.0.CO;2

[26] Nesbitt, R.W. and Sun, S.S. (1976) Geochemistry of Archaean Spinifex-Textured Peridotites and Magnesian and Low-Magnesian Tholeiites. *Earth and Planetary Science Letters*, **31**, 433-453. https://doi.org/10.1016/0012-821X(76)90125-4

[27] Sun, S. and McDonough, W. (1989) Chemical and Isotopic Systematics of Oceanic Basalts: Implications for Mantle Composition and Processes. In: Saunders, A.D. and Norry, M.J., Eds., *Magmatism in the Ocean Basins*, Geological Society of London, London, 313-345. https://doi.org/10.1144/GSL.SP.1989.042.01.19

[28] Kerrich, R. and Xie, Q. (2002) Compositional Recycling Structure of an Archean Super-Plume: Nb-Th-U-LREE Systematics of Archean Komatiites and Basalts Revisited. *Contributions to Mineralogy and Petrology*, **142**, 476-484. https://doi.org/10.1007/s004100100301